Wall Repulsion of Charged Colloidal Particles during Electrophoresis in Microfluidic Channels

Raúl Fernández-Mateo,[1] Víctor Calero,[2] Hywel Morgan,[1] Pablo García-Sánchez,[2] and Antonio Ramos[2,*]

[1] *School of Electronics and Computer Science, University of Southampton, Southampton SO17 1BJ, United Kingdom.*
[2] *Depto. Electrónica y Electromagnetismo. Facultad de Física. Universidad de Sevilla. Avda. Reina Mercedes s/n, 41012. Sevilla (Spain).*

Electrophoresis describes the motion of charged particles suspended in electrolytes when subjected to an external electric field. Previous experiments have shown that particles undergoing electrophoresis are repelled from nearby channel walls, contrary to the standard description of electrophoresis that predicts no hydrodynamic repulsion. Dielectrophoretic (DEP) repulsive forces have been commonly invoked as the cause of this wall repulsion. We show that DEP forces can only account for this wall repulsion at high frequencies of applied electric field. In the presence of a low-frequency field, quadrupolar electroosmotic flows are observed around the particles. We experimentally demonstrate that these hydrodynamic flows are the cause of the widely observed particle-wall interaction. This hydrodynamic wall repulsion should be considered in the design and application of electric-field driven manipulation of particles in microfluidic devices.

Electrophoresis is the motion of colloidal particles suspended in an aqueous electrolyte under the influence of spatially uniform electric fields [1]. The mechanism has been extensively exploited for analysis and separation of colloids and macromolecules such as DNA, RNA and proteins [2, 3]. Particles suspended in an electrolyte carry a net surface charge which is screened by a diffuse ionic layer on the electrolyte side of the interface. The action of an external electric field leads to a relative motion between the liquid and particle. The relation between the applied field $\mathbf{E}$ and the particle velocity $\mathbf{u}$ when the diffuse ionic layer is thin compared to the particle dimension was obtained by Smoluchowski [4]

$$\mathbf{u} = \frac{\varepsilon\zeta}{\eta}\mathbf{E} \tag{1}$$

where ε and η are the electrolyte permittivity and viscosity respectively, and ζ is the zeta potential of the particle-electrolyte interface. The latter is usually considered to be the electrical potential at the inner edge of the diffuse ionic layer surrounding the particle [1].

Combining electrokinetic forces with microfluidics has led to new methods for precise control of particles and liquids on the micro-scale [5, 6]. In many of these electrically-assisted microfluidic techniques, the interaction between the particles and the channel walls plays a significant role. In particular, multiple studies have shown that spherical particles undergoing electrophoresis are repelled from nearby dielectric walls [7, 8]. However, the classical theory of electrophoresis does not predict such repulsion (nor attraction) from the walls [9, 10]. According to theory, the velocity field around the particle scales linearly with the electric field amplitude. A simple symmetry argument leads to the conclusion that the particle velocity perpendicular to the wall is zero. Assuming that for a given electric field the particle is repelled from the wall, then upon a change of direction of the field, the velocity field will change direction and attraction to the wall is predicted. This leads to a paradox since both situations are equivalent.

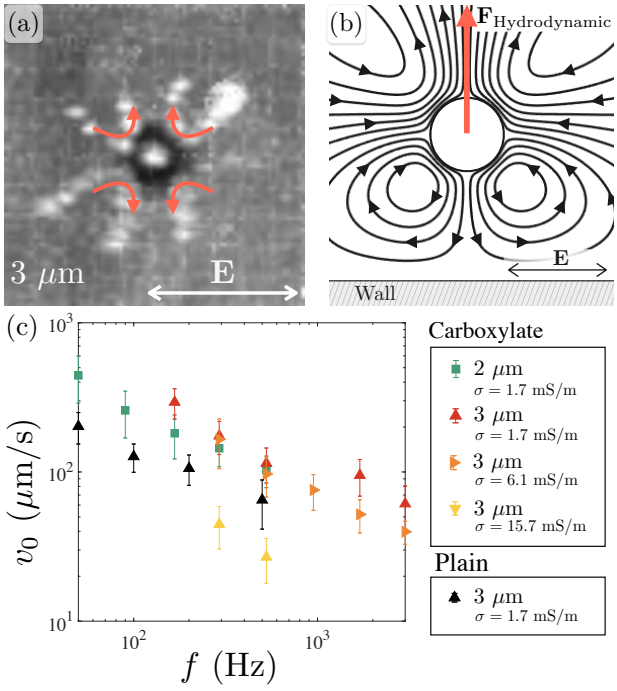

FIG. 1. (a) Experimental images of fluid flow around a single 3 μm diameter particle far from the wall. Flow was observed using 500 nm diameter tracer particles. The final image was created from a superposition of a stack of images and the arrows indicate the flow direction. The particle is suspended in KCl of $\sigma = 1.7$ mS/m and an AC field with a frequency of 200 Hz and amplitude of 80 kV/m. (b) Schematic diagram showing how this flow leads to particle-wall repulsion. (c) Experimental data of slip velocity on the particles v_0 versus frequency for an applied field with a magnitude of 80 kV/m.

* Corresponding author: ramos@us.es

Wall repulsion in electrophoresis has been explained in terms of a dielectrophoretic (DEP) repulsion [11], a force which scales quadratically with the electric field, and thus the symmetry argument above does not apply. DEP repulsion can be described in terms of the image charges associated with the insulating walls.

In this work we provide experimental evidence for wall-particle interaction in AC electric field of different frequencies, and demonstrate that DEP cannot account for the repulsion observed at low frequencies, which is much larger than predicted. We demonstrate that the main contribution to wall repulsion in electrophoresis arises from a stationary fluid flow around the particles.

We recently reported that AC electric fields induce stationary fluid flows around insulating charged cylinders [12, 13] and spheres [14]. These flows are referred to as concentration polarization electroosmosis (CPEO) since their origin is attributed to the perturbation of the slip velocity due to local variations in electrolyte concentrations arising from surface conduction. These CPEO flows are quadratic with the electric field and therefore have a non-zero time average, which is observed experimentally as a stationary flow. It therefore follows that particle repulsion from nearby walls must occur.

Figure 1(a) shows an example of the observed stationary flow around a 3 μm diameter microsphere suspended in KCl (1.7 mS/m) in the presence of an AC electric field with a frequency of 200 Hz and amplitude of 80 kV/m. The fluid patterns were observed using 500 nm diameter fluorescent beads that act as flow tracers. Taking the direction of the electric field as the polar axis, the liquid flows towards the particle at both poles and away from the particle at the equator. Figure 1(b) depicts how the liquid flow is driven from the particle towards the wall leading to a hydrodynamic repulsion. Figure 1 (c) shows experimental data of the slip velocity on the particles versus frequency for an applied field with a magnitude of 80 kV/m, (See Supplementary Materials for details).

The experimental devices were made from polydimethylsiloxane (PDMS) using standard soft-lithography and bonded to a glass wafer. They consisted of a 1 cm long channels with a 50×50 μm square cross-section - see Figure 2(a). Voltages were applied along the channel using two metal needles inserted into the reservoirs at each end. Electric fields were generated with an amplitude of 80 kV/m and frequencies ranging from 50 Hz to 10 kHz. The wall repulsion was measured for fluorescent carboxylate particles of 1 μm, 2 μm, and 3 μm diameter, along with 3 μm diameter plain polystyrene particles; these have a lower surface charge than the carboxylate particles. All particles were suspended in KCl solutions at conductivities of 1.7, 6.1, and 15.7 mS/m. Before the experiments, the channels were pre-treated with a non-ionic surfactant (Pluronic F-127) to avoid non-specific particle adhesion to the channel walls. A side-effect of this treatment is that electroosmosis on the channel walls is very much reduced [15, 16].

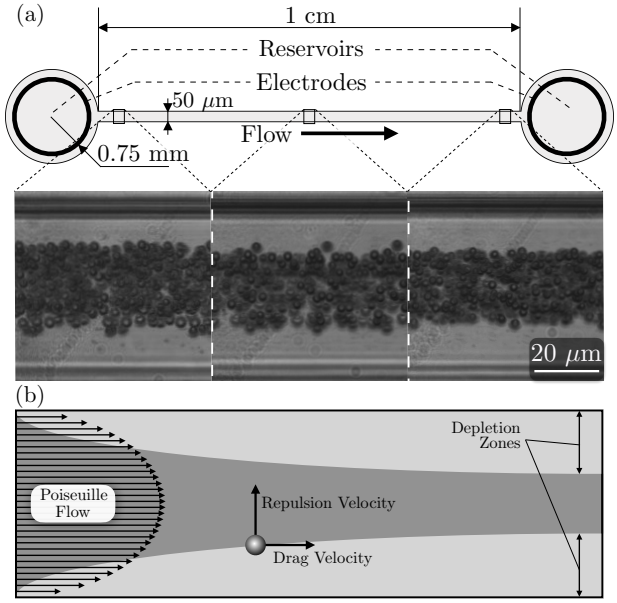

FIG. 2. (a) Schematic diagram of the experimental device (not to scale) and images of the observed particle wall repulsion at three different positions along the channel (3 μm plain particles, AC field at a frequency of 90 Hz and amplitude 80 kV/m, KCl electrolyte conductivity 6.1 mS/m). The images are obtained by superimposing frames of single particles. (b) Sketch of the expected behavior of the particles subjected to both a Poiseuille flow and a hydrodynamic wall repulsion.

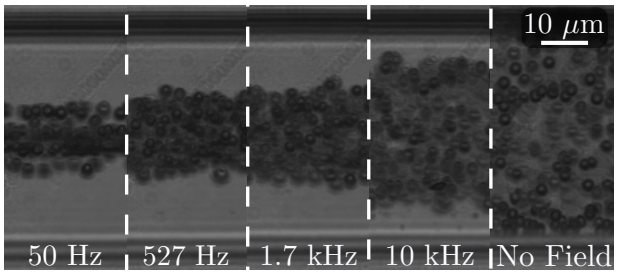

FIG. 3. Superimposed images at the end of the channel of 3 μm carboxylate particles suspended in 1.7 mS/m KCl solution for different frequencies. The electric field amplitude is 80 kV/m.

To begin with, particle-wall separation was investigated following the application of an AC electric field along the microchannel together with a pressure-driven flow with a maximum velocity of approximately 1.56 mm/s. The particle concentration was kept low so that particles flowed through the channel one by one, eliminating particle-particle interaction. When no electric field was applied, the particles were randomly distributed across the channel.

Figure 2(a) shows the repulsion from the wall at three different locations along the channel: immediately after the channel inlet, center and end of the channel. The images were obtained from the superimposition of more

than 600 frames of single particles in the pressure-driven flow. The applied field frequency was 90 Hz and the electrolyte conductivity was 6.1 mS/m. Particles enter the channel randomly distributed and the effect of the particle-wall repulsion leads to a particle-free region near the walls, as schematically shown in Figure 2(b). The width of the depleted region grows downstream but at a decreasing rate, indicating that the repulsion decays with distance from the wall.

The particle-wall repulsion data set is summarised in Figure 3. This shows the extent of the depletion region at the end of the microchannel as a function of electric field frequency. The wall repulsion is most significant at low frequencies and vanishes for high frequencies. To determine this separation, a custom software was used to plot a histogram of the transverse coordinates of each particle, i.e. the coordinate perpendicular to the channel wall z_i, $i \in (1, ..., N)$ where N the total number of particles counted. The mean particle-wall separation was determined as half the difference between the channel width and the width of the distribution of z_i (this width Δz is defined as the range that contains 95% of all particle positions). Further details are provided in the Supplementary Material.

Figure 4 shows the particle-wall separation as a function of electric field frequency. In all cases, wall separation decays with frequency. Figure 4(a) shows that this separation increases with particle size. It also shows that the separation for two particles with equal diameters is larger for the most charged, i.e. carboxylate spheres experience the greatest repulsion. Figure 4(b) shows that, for a given particle size, the separation decreases with electrolyte conductivity. The dashed lines in these figures indicate the calculated maximum particle-wall separation predicted by DEP repulsion according to Eq. (7). The experimental data clearly show that the calculated DEP force significantly underestimates the separation. However, for experimental conditions where CPEO flows vanish, a very good agreement with prediction due to DEP is found (see data at high frequencies in Figure 4(b) for the highest conductivity and in Figure 4(a) for plain particles).

As mentioned previously, we recently reported the presence of stationary CPEO flows around charged dielectric microspheres in the presence of an AC electric field [14]. The general trends observed for particle-wall separation in these experiments reported in Figure 4 mirror the characteristics of CPEO flows, which also decrease with electrolyte conductivity and frequency [13, 14]. In addition, a reduced concentration polarization and associated CPEO flow is expected for plain spheres, since particles with lower surface charge have a lower surface conductance. We propose that CPEO flows around individual particles are responsible for the observed particle-wall separation. To validate this hypothesis, a second set of experiments was conducted to quantify the strength of the quadrupolar flow velocity shown in figure 1(a). Fluorescent colloids (500 nm) were used as tracers to observe

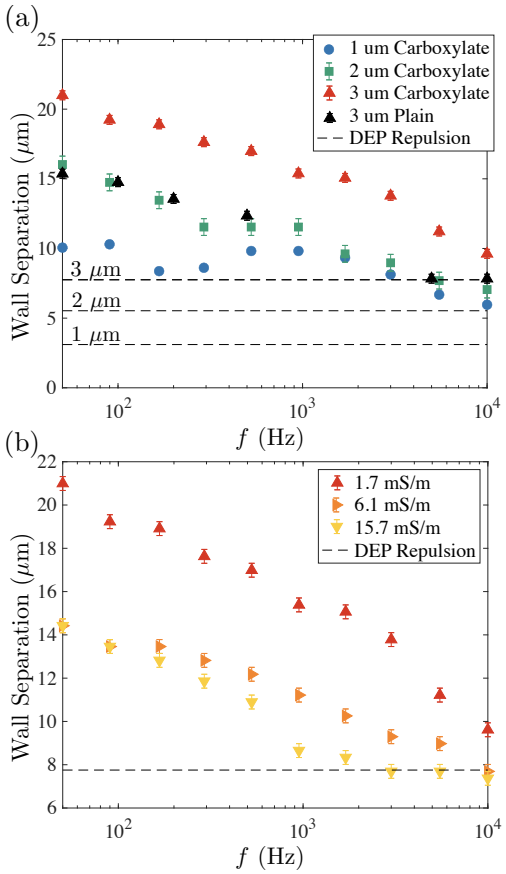

FIG. 4. Wall separation measured at the end of the channel for **(a)** different particles in an electrolyte of 1.7 mS/m conductivity; **(b)** different electrolyte conductivities for the 3 μm carboxylate beads. The wall separation represents the size of the depletion zones in Figure 3. Dashed lines represent the maximum separation predicted by dielectrophoresis, Eq. (7) with $\alpha = -0.5$.

the flow around particles far from the channel walls and in the absence of pressure-driven flow. Flow tracing was performed for three different populations of particles (2 μm carboxylate, 3 μm plain, and 3 μm carboxylate) suspended in the same 1.7 mS/m conductivity electrolyte and, also, for the 3 μm carboxylate in three different electrolyte conductivities (1.7, 6.1 and 15.7 mS/m KCl). Fluid flow was measured using computer-assisted Particle Image Velocimetry (PIV).

Theoretically, an axisymmetric flow is expected with the axis defined by the electric field direction, as in the flow pattern first predicted by Gamayunov et al. [17]:

$$\mathbf{v} = v_0 \left(\frac{(1-(r/a)^2)(1+3\cos 2\theta)}{2(r/a)^4} \hat{r} + \frac{\sin 2\theta}{(r/a)^4} \hat{\theta} \right), \quad (2)$$

where r and θ are, respectively, the radial distance and polar angle, a the sphere radius, and v_0 is the maximum time-averaged slip velocity at the particle surface. Thus, v_0 can be obtained as a single parameter from a least squares fit of Eq. (2) to the experimental velocity fields.

As expected, v_0 decreases with electrolyte conductivity and frequency of electric field, see Figure 1(c).

The distortion of this flow pattern by the presence of a wall can be calculated by the method of reflections [18]. In this case, the reflected flow leads to a net particle motion perpendicular to the wall. If the particle is far from the wall this velocity is given by:

$$\mathbf{u} = v_0 \frac{3a^2}{8h^2}\hat{z}, \tag{3}$$

where h is the distance of the particle center to the wall. This expression was obtained by Yariv [19] in the context of induced charge electroosmotic (ICEO) flows around conducting spheres, [20]. Equation (3) is the leading-order term in the method of reflections for small values of a/h. Eq. (3) can also be found from the image system of the fundamental singularities of Stokes' equations [21]. The expression by Gamayunov (2) reduces to a stresslet [22] with velocity field $\mathbf{v} = -v_0(1+3\cos 2\theta)/(2(r/a)^2)\hat{r}$ for $a/r \ll 1$. In the Supplementary Material the velocity field of this stresslet is calculated in the vicinity of a non-slip wall, and the velocity that is induced on the particle is given by equation (3).

An analytical expression for the particle wall-distance was obtained as follows. The fluid velocity in the middle horizontal plane of the channel (where the particles are imaged) is approximated by a parabolic profile,

$$\mathbf{v} = 4\mathcal{V}\left[\frac{z}{W} - \left(\frac{z}{W}\right)^2\right]\hat{x}, \tag{4}$$

where $\mathcal{V}$ is the maximum fluid velocity and W is the width of the channel. If the particle velocity perpendicular to the wall u_z is given by (3) and the longitudinal velocity u_x by (4), $\mathrm{d}z/\mathrm{d}x = u_z/u_x$ can be integrated to obtain the following expression that links the particle-wall separation h with the time-average slip velocity at the particle surface v_0 after covering a distance L along the channel:

$$\frac{v_0 a^2 L}{\mathcal{V}W^3} = \frac{8}{15}\left[5\left(\frac{h}{W}\right)^4 - 4\left(\frac{h}{W}\right)^5\right]. \tag{5}$$

Use of equation (5) assumes that the remote-wall approximation that leads to Eq. (3) is valid, i.e. higher order terms are neglected. To confirm this assumption, we have numerically calculated the velocity component perpendicular to the wall of a sphere, with a slip velocity given by $\mathbf{v}_s = v_0 \sin 2\theta\ \hat{\theta}$. By integrating this velocity, the particle-wall separation is found, and comparison with the prediction of (5) shows a negligible difference for $h \gg a$ (see Supplementary Material).

The wall repulsion due to DEP was calculated using the method of images for an insulating wall. The repulsion velocity due to this mechanism far from the wall is:

$$u_{\mathrm{DEP}} = \frac{\varepsilon a^5 (\alpha E_0)^2}{16\eta h^4} \tag{6}$$

where α is the real part of the non-dimensional polarizability, which for a sphere ranges between -0.5 and 1 [23]. The wall separation due to DEP satisfies:

$$\frac{\varepsilon a^5 L(\alpha E_0)^2}{\mathcal{V}W^5\eta} = \frac{32}{21}\left[7\left(\frac{h}{W}\right)^6 - 6\left(\frac{h}{W}\right)^7\right]. \tag{7}$$

For comparison with the experimental wall separation, a non-dimensional polarizability $\alpha = -0.5$ was used, which corresponds to the maximum polarizability in absolute value for a particle that is less polarizable than the medium. Note that the repulsion velocity generated by DEP decays as $(a/h)^4$, while the repulsion generated by the CPEO flow decays as $(a/h)^2$. Thus, DEP repulsion is a much shorter range effect.

Figure 5 shows the wall-separation (data in Figure 4) for a given particle versus its slip velocity v_0 (data in Figure 1(c)) measured under the same experimental conditions (i.e. electrolyte conductivity, amplitude and frequency of electric field). Wall-separations and v_0 are, respectively, scaled with channel width W and $a^2L/\mathcal{V}W^3$. The figure shows how the experimental data collapse onto a single (solid) line, which corresponds to the prediction given by Eq. (5). This result means that, irrespective of liquid conductivity, AC electric field, zeta potential or particle diameter, the separation is only determined by the product of $v_0 a^2$, i.e. the intensity of the stresslet. The dashed line depicts the separation for the case of maximum DEP-repulsion as calculated from Eq. (7).

Liang et al. [7] reported lateral migration of particles in a rectangular channel with electrophoresis and attributed this to DEP wall repulsion. However, their experimental data shows separation that was systematically greater than that predicted by DEP. Kazoe et al. [24] also reported wall-separation induced by DC electric fields for sub-micron particles (100- 900nm diameter) and concluded that the particle-wall force was around 40 times larger than DEP force. Experiments with DC electrophoresis show that wall repulsion decreases with electrolyte conductivity [8], and the importance of zeta potential and surface conductance has been emphasized [8, 25, 26] in agreement with our findings. It is also important to note that inertial lift in shear flows is affected by electrophoresis, as demonstrated by Lochab et al. [27]. However, the Reynolds number in our experiments is around 0.05 so that inertial effects can be safely neglected.

In conclusion, experimental data demonstrates that wall repulsion in AC electrophoresis is due to the presence of a stationary fluid flow around microparticles that is induced by an applied electric field. The origin of these flows is attributed to the perturbation of the electroosmotic slip velocity due to concentration polarization arising from surface conductance. Consequently, and in contrast to the widely reported common hypothesis, our analysis demonstrates that DEP is not the main contribution to particle wall repulsion for electrophoresis at low frequencies (below 10 kHz for our experimental conditions). This phenomenon will have consequences for

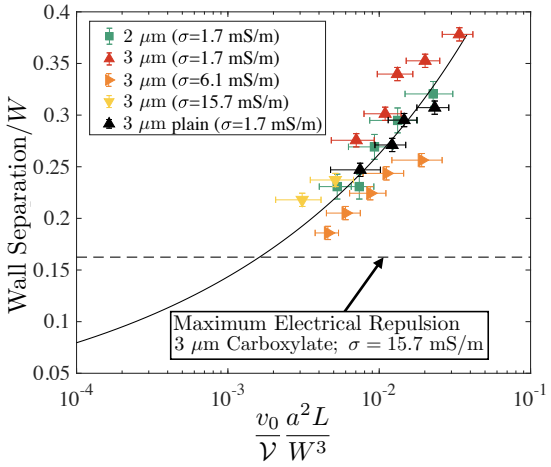

FIG. 5. Nondimensional wall separation versus nondimensional slip velocity. The figure shows experimental values of wall separation versus experimental values of slip velocity. They follow the trend predicted by Eq. (5). The dashed horizontal line represents the maximum electrical repulsion calculated from eq. (7)

the design of microfluidic technologies which use electric fields for particle manipulation and separation [26]. For example, particle manipulation by Deterministic Lateral Displacement [28], insulating DEP [29] and colloidal assembly [30] all make use of low frequency electric fields and the behaviour will be unavoidably influenced by the CPEO flows.

ACKNOWLEDGMENTS

PGS and AR acknowledge financial support by ERDF and Spanish Research Agency MCI under contract PGC2018-099217-B-I00.

[1] R. Hunter, *Introduction to Modern Colloid Science* (Oxford University Press, 1993).
[2] J.-L. Viovy, Reviews of Modern Physics **72**, 813 (2000).
[3] P. H. O'Farrell, Journal of biological chemistry **250**, 4007 (1975).
[4] M. von Smoluchowski, Bull. Akad. Sci. Cracovie. **8**, 182 (1903).
[5] H. Morgan and N. G. Green, *AC Electrokinetics: colloids and nanoparticles.* (Research Studies Press Ltd., 2003).
[6] D. J. Harrison, K. Fluri, K. Seiler, Z. Fan, C. S. Effenhauser, and A. Manz, Science **261**, 895 (1993).
[7] L. Liang, Y. Ai, J. Zhu, S. Qian, and X. Xuan, Journal of colloid and interface science **347**, 142 (2010).
[8] Z. Liu, D. Li, Y. Song, X. Pan, D. Li, and X. Xuan, Physics of Fluids **29**, 102001 (2017).
[9] H. J. Keh and J. L. Anderson, Journal of Fluid Mechanics **153**, 417 (1985).
[10] H. J. Keh and S. B. Chen, Journal of Fluid Mechanics **194**, 377 (1988).
[11] E. Yariv, Soft Matter **12**, 6277 (2016).
[12] V. Calero, P. Garcia-Sanchez, A. Ramos, and H. Morgan, Journal of Chromatography A , 461151 (2020).
[13] V. Calero, R. Fernández-Mateo, H. Morgan, P. García-Sánchez, and A. Ramos, Physical Review Applied **15**, 014047 (2021).
[14] R. Fernández-Mateo, P. García-Sánchez, V. Calero, H. Morgan, and A. Ramos, Journal of Fluid Mechanics **924** (2021).
[15] M. Viefhues, S. Manchanda, T.-C. Chao, D. Anselmetti, J. Regtmeier, and A. Ros, Analytical and bioanalytical chemistry **401**, 2113 (2011).
[16] R. Fernández-Mateo, P. García-Sánchez, V. Calero, A. Ramos, and H. Morgan, Electrophoresis.
[17] N. I. Gamayunov, V. A. Murtsovkin, and A. S. Dukhin, Colloid J. USSR (Engl. Transl.) **48**, 197 (1986).
[18] J. Happel and H. Brenner, *Low Reynolds number hydrodynamics: with special applications to particulate media*, Vol. 1 (Springer Science & Business Media, 2012).
[19] E. Yariv, Proceedings of the Royal Society A: Mathematical, Physical and Engineering Sciences **465**, 709 (2009).
[20] ICEO flows are negligible for dielectric particles [12] and, therefore, the origin of the quadrupolar flows is attributed to CPEO.
[21] J. Blake and A. Chwang, Journal of Engineering Mathematics **8**, 23 (1974).
[22] G. Batchelor, Journal of Fluid Mechanics **44**, 419 (1970).
[23] T. B. Jones, *Electromechanics of Particles* (Cambridge University Press, 1995).
[24] Y. Kazoe and M. Yoda, Langmuir **27**, 11481 (2011).
[25] Z. Liu, D. Li, M. Saffarian, T.-R. Tzeng, Y. Song, X. Pan, and X. Xuan, Electrophoresis **40**, 955 (2019).
[26] C. Thomas, X. Lu, A. Todd, Y. Raval, T.-R. Tzeng, Y. Song, J. Wang, D. Li, and X. Xuan, Electrophoresis **38**, 320 (2017).
[27] V. Lochab and S. Prakash, Soft Matter **17**, 611 (2021).
[28] V. Calero, P. Garcia-Sanchez, C. Honrado, A. Ramos, and H. Morgan, Lab on a Chip **19**, 1386 (2019).
[29] E. B. Cummings and A. K. Singh, Analytical chemistry **75**, 4724 (2003).
[30] M. Trau, D. A. Saville, and I. A. Aksay, Langmuir **13**, 6375 (1997).